Contemporary Mathematics
http://ojs.wiserpub.com/index.php/CM/

Research Article

Digital Image Processing Using Coefficients of Sakaguchi Kind Function Defined in Limacon Shaped Domain with Power Law Transformation

Priya H, Sruthakeerthi B*

Department of Mathematics, School of Advanced Sciences, Vellore Institute of Technology, Chennai, Tamilnadu, India
E-mail: sruthakeerthi.b@vit.ac.in

Received: 21 February 2024; **Revised:** 1 July 2024; **Accepted:** 11 July 2024

Abstract: Digital image processing is a constantly evolving field that focuses on digital image analysis, enhancement, and modification. Another popular approach used to improve the aesthetic appeal and diagnostic usefulness of images is power law transformation. Power law transformation and the analysis of analytic coefficients obtained from complex functions within digital image processing have become more popular recently. We demonstrate that analytic coefficients provide a solid foundation for investigating phase information in images and enhancing certain aspects of images. Complex image processing tasks, like spatial filtering, picture segmentation, and contrast enhancement, can be efficiently completed by combining power law transformation with analytical coefficients. This study focuses on applying analytic coefficients that come from a specific group of Sakaguchi-type functions are used to improve images by transmitting to a domain shaped like a Limacon. The article also provides a wide range of instances that highlight the usefulness of this method in the field of medical imaging. The results unequivocally highlight the significance of analytic coefficients and power law transformation as valuable tools for digital image processing.

***Keywords*:** analytic function, subordination, image enhancement, image quality, quality metrics

MSC: 30C45, 30C50

Abbreviation

DIP	Digital Image Processing
MSE	Mean-Square Error
PSNR	Peak-Signal-to-Noise Ratio
SSIM	Structural Similarity Index Measure
AMBE	Absolute Mean Brightness Error
MRI	Magnetic Resonance Imaging
CT	Computed Tomography

DOI: https://doi.org/10.37256/cm.5320244489

1. Introduction

The article discusses mathematical findings from the geometric function theory and sheds light on how it is used in DIP. Due to its significance in conformal mapping that locally preserves angles, the limacon-shaped domain is taken into consideration in this work. The aforementioned domain is crucial for region of interest extraction, shape analysis, image transformation, filtering, and enhancement, as well as geometric image representation and registration, all of which are aspects of image processing. To accomplish particular image processing objectives, these techniques make use of the peculiar characteristics of limacon-shaped domains. The momentum of this article is to improve clarity by offering a provocative option for image processing.

The term "digital image processing" describes the use of mathematical techniques to modify digital images. It includes methods for improving, modifying, and analysing digital images for a range of purposes, including feature extraction, image restoration, image segmentation, image compression, and pattern recognition. Computers are used in digital image processing to execute operations on digital images that can be obtained from a variety of sources, including digital cameras, scanners, and medical imaging equipment. Each value in the arrays of numerical values that make up the images represents a pixel in the image. In many multiple industries, including medicine, remote sensing, computer vision, and entertainment, digital image processing has numerous useful implications. For instance, it is possible to analyse satellite images to discover land use trends and medical imaging to extract information that is helpful for diagnosis. Image enhancement, a crucial component of digital image processing, tries to raise the calibre of an image by modifying its elements to make it more aesthetically pleasing or simpler to comprehend. Following are some justifications for why image improvement is crucial: Improve visual quality, Enhance details, Remove noise, Correct brightness and contrast and Aid in analysis.

1.1 *Power law transformation in DIP*

When adjusting the contrast of images, power law transformation is a typical technique in digital image processing. It is often referred to as gamma transformation or gamma correction. The following is a definition of the power law transformation function:

$$s = cr^{\gamma},$$

where

$s =$ output pixel value.

$r =$ input pixel value.

$\gamma =$ gamma value.

$c =$ constant.

Gamma values less than 1 decrease the contrast of the image, while values greater than 1 increase the contrast. By altering the mapping of input pixel values to output pixel values, power law transformation is used to adjust the brightness and contrast of an image. This method is especially helpful when the image's dynamic range is either too low or too high for analysis or display. For instance, in dim lighting, an image could appear overly dark and lacklustre. The brightness and contrast of a power law transformation with a gamma value larger than 1 can be increased, improving the visibility of the image. Similar to this, an image may seem overexposed and overly brilliant in high light situations. By reducing the brightness and enhancing the contrast with a power law transformation, the image can be made more visually appealing.

The effectiveness of image enhancement methods like power law transformation is assessed in digital image processing using quality metrics. Here there are a few typical quality metrics for rating the effectiveness of power law transformation: MSE, PSNR, SSIM, AMBE and Entropy.

Image filtering is one of the primary uses of analytical coefficients in DIP. Complex filtering procedures like phase shifting, frequency translation, and frequency domain filtering can be carried out using analytical coefficients. Edges, textures, and regions of interest can all be improved or altered in an image by applying these operations on the analytic

coefficients. The ability to selectively modify specific image attributes is one of the key benefits of utilising analytical coefficients for image enhancement. It is possible to recognise and improve particular features in the image, such as edges, textures, and regions of interest, by evaluating the phase information in the analytic coefficients. To accomplish the required augmentation, this can be done using a variety of filtering approaches, such as homomorphic filtering or phase-only filtering, which alter the magnitude and phase of the analytic coefficients.

1.1.1 *Power law transformation's contribution in the realm of medicine*

Power law transformation is a type of image enhancement technique that is commonly used in medical imaging to improve the visual quality and diagnostic accuracy of medical images. There are several reasons why power law transformation is an important technique for medical image enhancement:

Non-linear contrast adjustment: Power law transformation is a non-linear technique that allows for contrast adjustment in a way that is different from linear techniques such as histogram equalization. This is particularly important in medical imaging where subtle variations in contrast can be critical for diagnosis.

Retention of image information: Power law transformation preserves the original information in the image, while enhancing its contrast. This is important in medical imaging where it is important to retain as much information as possible, while still improving the quality of the image.

Flexibility in adjustment: The power law transformation parameter (gamma) can be adjusted to obtain different levels of enhancement. This allows the technique to be tailored to the specific requirements of different imaging modalities and applications.

Compatibility with other enhancement techniques: Power law transformation can be combined with other enhancement techniques such as spatial filtering, Fourier transformation, and wavelet transformation to achieve more advanced image processing tasks.

Speed: Power law transformation is a fast technique that can be implemented in real-time, making it well-suited for medical imaging applications where quick and accurate diagnoses are critical.

In this study, we offer a novel method for improving images based on the coefficients obtained by Sakaguchi kind of function defined in Limacon shaped domain. The remainder of this research is structured as: Section 2 covers the mathematical approach, Section 3 delves into the application of the coefficients calculated, Section 4 provides conclusion of the entire article and finally Section 5 throws limelight for future work.

2. Mathematical approach

Let $\mathscr{A}$ be analytic of the form:

$$f(\xi) = \xi + \sum_{\kappa=2}^{\infty} a_{\kappa}\xi^{\kappa}, \quad \xi \in \mathbb{U}, \tag{1}$$

in $\mathbb{U} = \{\xi \in \mathbb{C} : |\xi| < 1\}$. Ma and Minda [1] amalgamated various subclasses of starlike and convex functions which are subordinate to a function $\psi \in \mathfrak{P}$ ($\mathfrak{P}$ be the class of functions with positive real part consisting of all analytic functions $p : \mathbb{U} \to \mathbb{C}$ satisfying $p(0) = 1$ and $\mathscr{R}p(\kappa) > 0$) with $\psi(0) = 1$, $\psi'(0) > 0$, ψ maps $\mathbb{U}$ onto a region starlike with respect to 1 and symmetric with respect to real axis and familiarized the classes as below:

$$\mathscr{S}^{*}(\psi) = \left\{ f \in \mathscr{A} : \frac{\xi f'(\xi)}{f(\xi)} \prec \psi \right\}, \tag{2}$$

and

$$\mathscr{C}(\psi)=\left\{f\in\mathscr{A}:1+\frac{\xi f''(\xi)}{f'(\xi)}\prec\psi\right\}. \tag{3}$$

Similarly many authors [2–5] studied for different domains. The equation of cardioid

$$(9x^2+9y^2-18x+5)^2-16(9x^2+9y^2-6x+1)=0, \tag{4}$$

was studied in [6]. Lately, [7] introduced $ST_{L(s)}$ and $CV_{L(s)}$ respectively. Geometrically, $f\in\mathscr{A}$ such that $\frac{\xi f'(\xi)}{f(\xi)}$ and $\frac{(\xi f'(\xi))'}{f'(\xi)}$, respectively, are in

$$[(u-1)^2+v^2-s^4]^2=4s^2[(u-1+s^2)^2+v^2], \tag{5}$$

where

$$L_s(z=e^{i\theta})=(1+se^{i\theta})^2=(1+s(cos\theta+isin\theta))^2=u+iv,$$

$$1+2s(cos\theta+isin\theta)+s^2(cos^2\theta+2icos\theta sin\theta-2sin^2\theta)=u+iv,$$

$$u=1+2scos\theta+s^2cos2\theta,$$

$$v=2ssin\theta(1+scos\theta),$$

where $u=u(\theta)$, $v=v(\theta)$ and $0<s\leq\frac{1}{\sqrt{2}}$.

Lately, [8] defined the bean-shaped:

$$\Omega(\mathbb{U})=\{w=x+iy:(4x^2+4y^2-8x-5)^2+8(4x^2+4y^2-12x-3)=0\}, \tag{6}$$

where $s\in[-1,\ 1]\setminus\{0\}$.

If

$$\varphi(\xi):\mathbb{U}\to\mathbb{C}, \tag{7}$$

is the function defined by

$$\varphi(\xi)=1+\sqrt{2}\xi+\frac{1}{2}\xi^2, \tag{8}$$

is preferred [8].

Definition 1 Let $\varphi : \mathbb{U} \to \mathbb{C}$ be analytic and for $0 \leq \Lambda \leq 1$ and $0 \leq \tau \leq 1$ but $|\tau| \neq 1$, we let the class as

$$SC(\vartheta,\ \Lambda) = \left\{ f \in \mathscr{A} : \frac{(1-\tau^2)[\Lambda\xi^2 f''(\xi) + \xi f'(\xi)]}{\Lambda\xi[f'(\xi) - \tau f'(\tau\xi)] + (1-\Lambda)[f(\xi) - f(\tau\xi)]} \prec \varphi(\xi) \right\}, \tag{9}$$

where $\xi \in \mathbb{U}$ and $\varphi(\xi) = 1 + \sqrt{2}\xi + \frac{1}{2}\xi^2$.

Lemma 1 See [9]. Suppose that $p(\xi) = 1 + c_1\xi + c_2\xi^2 + \cdots$, $(\mathscr{R}p_1 > 0)$, $\xi \in \mathbb{U}$, then

$$|c_n| \leq 2 \ \ (n = 1,\ 2,\ 3,\ ...),$$

$$|c_2 - \nu c_1^2| \leq 2\ max\{1,\ |2\nu - 1|\},$$

and the outcome is sharp for the functions formulated by

$$p_1(\xi) = \frac{1+\xi^2}{1-\xi^2},$$

$$p_1(\xi) = \frac{1+\xi}{1-\xi}.$$

Lemma 2 See [1]. Suppose that $p_1(\xi) = 1 + c_1\xi + c_2\xi^2 + \cdots$, $(\mathscr{R}p_1 > 0)$, $\xi \in \mathbb{U}$. Then,
(i)

$$|c_2 - \nu c_1^2| \leq \begin{cases} -4\nu + 2 & \text{if } \nu \leq 0, \\ 2 & \text{if } 0 \leq \nu \leq 1, \\ 4\nu - 2 & \text{if } \nu \geq 1. \end{cases}$$

For $\nu < 0$ or $\nu > 1$, equality occurs when $p_1(\xi) = \frac{1+\xi}{1-\xi}$ or one of its rotations. When $\nu = 1$, equality holds if and only if $p_1(\xi)$ is the reciprocal of one of the functions such that equality holds in the case of $\nu = 0$.

(ii) For $\nu \in (0,\ 1)$, the equality exists when $p_1(\xi) = \frac{1+\xi^2}{1-\xi^2}$ or one of its rotations.

(iii) For $\nu = 0$, the equality happens when

$$p_1(\xi) = \left(\frac{1}{2} + \frac{1}{2}\vartheta\right)\frac{1-\xi}{1+\xi} + \left(\frac{1}{2} - \frac{1}{2}\vartheta\right)\frac{1-\xi}{1+\xi},$$

where $0 \leq \vartheta \leq 1$ or one of its rotations.

Lemma 3 See [10]. If $p \in \mathscr{P}$ and is given by $p(\xi) = 1 + c_1\xi + c_2\xi^2 + \cdots$ then

$$2c_2 = c_1^2 + x(4-c^2), \tag{10}$$

$$4c_3 = c_1^2 + 2(4-c_1^2)c_1x - c_1(4-c_1^2)x^2 + 2(4-c_1^2)(1-|x|^2\xi), \tag{11}$$

for some x, ξ with $|x| \leq 1$ and $|\xi| \leq 1$.

Theorem 1 Let the function $f \in SC(\vartheta,\ \Lambda)$ be given by (1) then

$$|a_2| \leq \frac{\sqrt{2}}{(1+\Lambda)(2-\varsigma_2)},$$

$$|a_3| \leq \frac{\sqrt{2}}{(1+2\Lambda)(3-\varsigma_3)}\ \ max\left\{1,\ \left|\frac{1}{2\sqrt{2}} + \frac{\sqrt{2}\varsigma_2}{2-\varsigma_2}\right|\right\} = \frac{\sqrt{2}}{(1+2\Lambda)(3-\varsigma_3)}\left(\frac{1}{2\sqrt{2}} + \frac{\sqrt{2}\varsigma_2}{2-\varsigma_2}\right).$$

Proof. Since $f \in SC(\vartheta,\ \Lambda)$, there exists w with $w(0) = 0$ and $|w(\xi)| < 1$ in $\mathbb{U}$ such that

$$\frac{(1-\tau^2)[\Lambda\xi^2 f''(\xi) + \xi f'(\xi)]}{\Lambda\xi[f'(\xi) - \tau f'(\tau\xi)] + (1-\Lambda)[f(\xi) - f(\tau\xi)]} = \varphi(w(\xi)). \tag{12}$$

Defining the function p_1,

$$p_1(\xi) = \frac{1+w(\xi)}{1-w(\xi)} = 1 + c_1\xi + c_2\xi^2 + \cdots, \tag{13}$$

or equivalently

$$w(\xi) = \frac{p_1(\xi)-1}{p_1(\xi)+1},$$

$$= \frac{1}{2}\left[c_1\xi + \left(c_2 - \frac{c_1^2}{2}\right)\xi^2 + \left(c_3 - c_1c_2 + \frac{c_1^3}{4}\right)\xi^3 + \cdots\right],$$

then p_1 is analytic in $\mathbb{U}$ with $p_1(0) = 1$ and has a positive real part in $\mathbb{U}$. By using the above equation with (8)

$$\begin{aligned}\varphi(w(\xi)) = \varphi\left(\frac{p_1(\xi)-1}{p_1(\xi+-1}\right) = 1 + \frac{c_1\xi}{\sqrt{2}} + \left(\frac{1}{\sqrt{2}}\left(c_2 - \frac{c_1^2}{2}\right) + \frac{c_1^2}{8}\right)\xi^2 \\ + \left\{\frac{1}{\sqrt{2}}\left(c_3 - c_1c_2 + \frac{c_1^2}{4}\right) + \frac{c_1}{4}\left(c_2 - \frac{c_1^2}{2}\right)\right\}\xi^3 + \cdots\end{aligned} \tag{14}$$

Since,

$$\frac{(1-\tau^2)[\Lambda\xi^2 f''(\xi)+\xi f'(\xi)]}{\Lambda\xi[f'(\xi)-\tau f'(\tau\xi)]+(1-\Lambda)[f(\xi)-f(\tau\xi)]}$$

$$= 1+\left[\frac{c_1}{\sqrt{2}}+a_2\varsigma_2(1+\Lambda)\right]\xi$$

$$+\left[\frac{1}{\sqrt{2}}\left(c_2-\frac{c_1^2}{2}\right)+\frac{c_1^2}{8}+\frac{c_1}{\sqrt{2}}a_2\varsigma_2(1+\Lambda)+a_3\varsigma_3(1+2\Lambda)\right]\xi^2 \tag{15}$$

$$+\left[\frac{1}{\sqrt{2}}\left(c_3-c_1c_2+\frac{c_1^3}{4}\right)+\frac{c_1}{4}\left(c_2-\frac{c_1^2}{2}\right)+a_2\varsigma_2(1+\Lambda)\left(\frac{1}{\sqrt{2}}\left(c_2-\frac{c_1^2}{2}\right)+\frac{c_1^3}{8}\right)\right.$$

$$\left.+\frac{c_1}{\sqrt{2}}a_3\varsigma_3(1+2\Lambda)+a_4\varsigma_4(1+3\Lambda)\right]\xi^3,$$

and equating the coefficients of ξ, ξ^2, ξ^3 from (14) to (15), we get

$$a_2=\frac{c_1}{\sqrt{2}(1+\Lambda)(2-\varsigma_2)}, \tag{16}$$

$$a_3=\frac{1}{4(1+2\Lambda)(3-\varsigma_3)}\left\{\left(\frac{1-2\sqrt{2}}{2}+\frac{2\varsigma_2}{2-\varsigma_2}\right)c_1^2+2\sqrt{2}c_2\right\}, \tag{17}$$

$$a_4=\frac{1}{16(1+3\Lambda)(4-\varsigma_4)}\left\{\left[2(\sqrt{2}-1)+\frac{\sqrt{2}(1-2\sqrt{2})\varsigma_2}{2-\varsigma_2}+\frac{8\sqrt{2}\varsigma_3}{3-\varsigma_3}\left(\frac{1-2\sqrt{2}}{8}+\frac{\varsigma_2}{2(2-\varsigma_2)}\right)\right]c_1^3\right.$$

$$\left.+\left[4(1-2\sqrt{2})+\frac{8\varsigma_2}{2-\varsigma_2}+\frac{8\varsigma_3}{3-\varsigma_3}\right]c_1c_2+8\sqrt{2}c_3\right\}. \tag{18}$$

Now applying Lemma 1, we get

$$|a_2|\leq\frac{\sqrt{2}}{(1+\Lambda)(2-\varsigma_2)}, \tag{19}$$

and also

$$|a_3| = \frac{1}{4(1+2\Lambda)(3-\varsigma_3)}\left|\left\{\left(\frac{1-2\sqrt{2}}{2}+\frac{2\varsigma_2}{2-\varsigma_2}\right)c_1^2+2\sqrt{2}c_2\right\}\right|,$$

$$= \frac{1}{\sqrt{2}(1+2\Lambda)(3-\varsigma_3)}\left|c_2-\left(\frac{2\sqrt{2}-1}{4\sqrt{2}}-\frac{\varsigma_2}{\sqrt{2}(2-\varsigma_2)}\right)c_1^2\right|, \tag{20}$$

$$= \frac{1}{\sqrt{2}(1+2\Lambda)(3-\varsigma_3)}|c_2-\kappa c_1^2|,$$

where $\kappa = \frac{2\sqrt{2}-1}{4\sqrt{2}} - \frac{\varsigma_2}{\sqrt{2}(2-\varsigma_2)}$. Now by applying Lemma 1, we get

$$|a_3| \leq \frac{\sqrt{2}}{(1+2\Lambda)(3-\varsigma_3)}\, max\left\{1,\ \left|\frac{1}{2\sqrt{2}}+\frac{\sqrt{2}\varsigma_2}{2-\varsigma_2}\right|\right\} = \frac{\sqrt{2}}{(1+2\Lambda)(3-\varsigma_3)}\left(\frac{1}{2\sqrt{2}}+\frac{\sqrt{2}\varsigma_2}{2-\varsigma_2}\right). \tag{21}$$

3. Application

This section seeks to show that the suggested image enhancement algorithm based on Power Law Transformation is validated using the coefficients found in the above section. By assigning suitable values to the parameters Λ, ς_2 and ς_3 to be 0, 1 and 1 respectively we obtain a numerical value for a_1, a_2 and a_3 as 1, 1.4142 and 1.2500 respectively. With the values obtained we design three outcomes, they are as follows:

Outcome 1: $s = cr^{a_1}$.

Outcome 2: $s = cr^{a_2}$.

Outcome 3: $s = cr^{a_3}$.

In the research findings, each image was examined with respect to each Outcome, and the average was also taken into account. Better outcomes are obtained for our model and at the average with regard to the constraints of the quality metrics considered. Using MATLAB R2021a and specially written code that takes into account the time and space complexity, the entire enhancement process is carried out and the obtained results are discussed in the Research Outcomes section and the algorithm is presented in Algorithm 1.

Algorithm 1

1. Load the test image into a variable 'I'.
2. Convert the image into grayscale image.
3. Assign variable 'B' to the grayscale image.
4. Convert 'B' to double precision.
5. Perform the proposed enhancement technique using the coefficients as gamma values.
6. Compute quality metrics (PSNR, SSIM, MSE, AMBE and Entropy).
7. Calculate the average result of three different outcomes.
8. Record the numerical results rounded to four decimal places.
9. Display the resulting images along with the original image.

3.1 *Research outcomes*

In this study, we examine MRI scans of three different breasts with malignant neoplasms and analyse the image using our suggested model to see if it performs well over a range of images. The images under consideration are 527×447, 467

$\times$ 522, and 367 $\times$ 385 pixels in size, respectively. The image that was obtained after using our algorithm has significantly clearer tumour cells, making it easier for doctors to diagnose the tumor's intensity.

The original image is presented along with the three outcomes are displayed in Figure 1, 2 and 3 and the values that were determined for the quality measures are given in Table 1, 2 and 3 respectively.

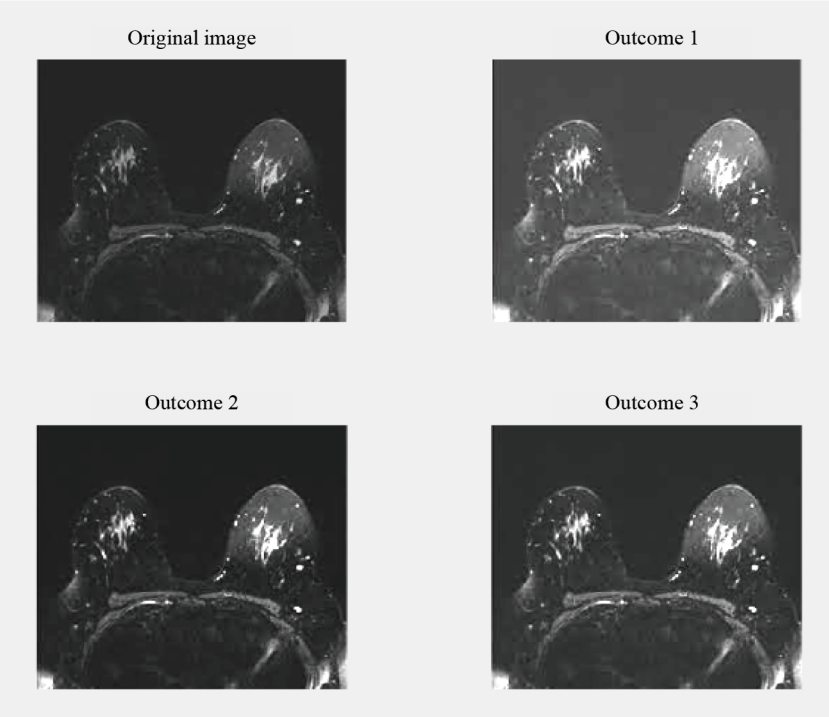

Figure 1. MRI of breast with malignant neoplasms image 1

Table 1. Values of the quality metrics obtained for different outcomes of image 1

Quality metrics	PSN	SSIM	MSE	AMBE	Entropy
Power law transformation: Outcome 1	13.9276	0.0047	2.6322×10^3	46.8317	4.6999
Power law transformation: Outcome 2	13.9047	0.0034	2.6461×10^3	47.0093	4.7643
Power law transformation: Outcome 3	13.9094	0.0036	2.6432×10^3	46.9534	4.7495
Average	13.9139	0.0039	2.6405×10^3	46.9315	4.7379

Table 2. Values of the quality metrics obtained for different outcomes of image 2

Quality metrics	PSNR	SSIM	MSE	AMBE	Entropy
Power law transformation: Outcome 1	14.4841	0.3282	2.3157×10^3	29.6434	5.3275
Power law transformation: Outcome 2	14.4661	0.3273	2.3252×10^3	29.7415	5.1607
Power law transformation: Outcome 3	14.4729	0.3276	2.3216×10^3	29.7105	5.3281
Average	14.4744	0.3277	2.3208×10^3	29.6985	5.2721

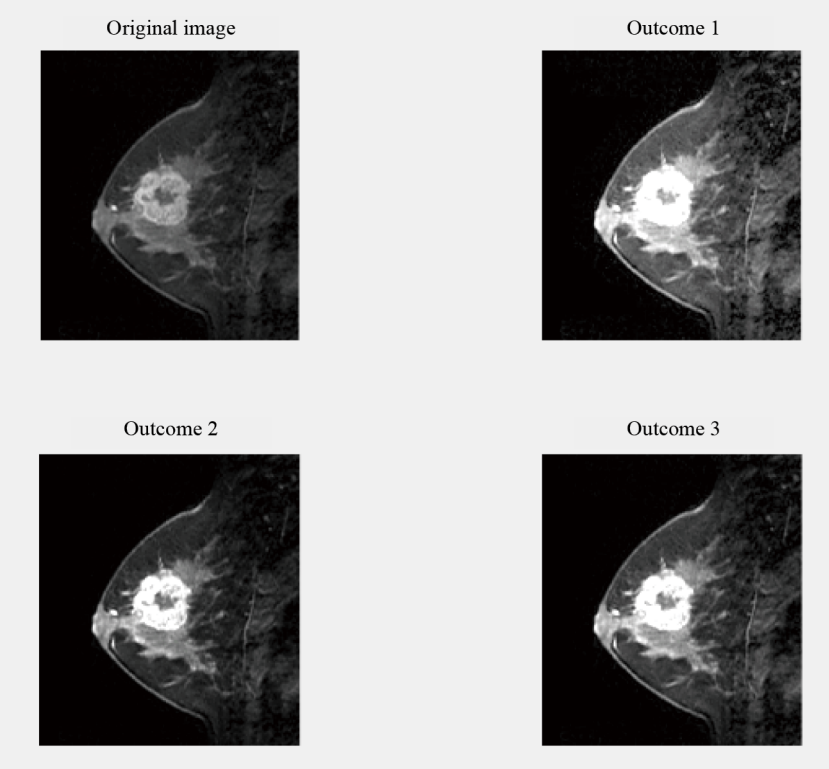

Figure 2. MRI of breast with malignant neoplasms image 2

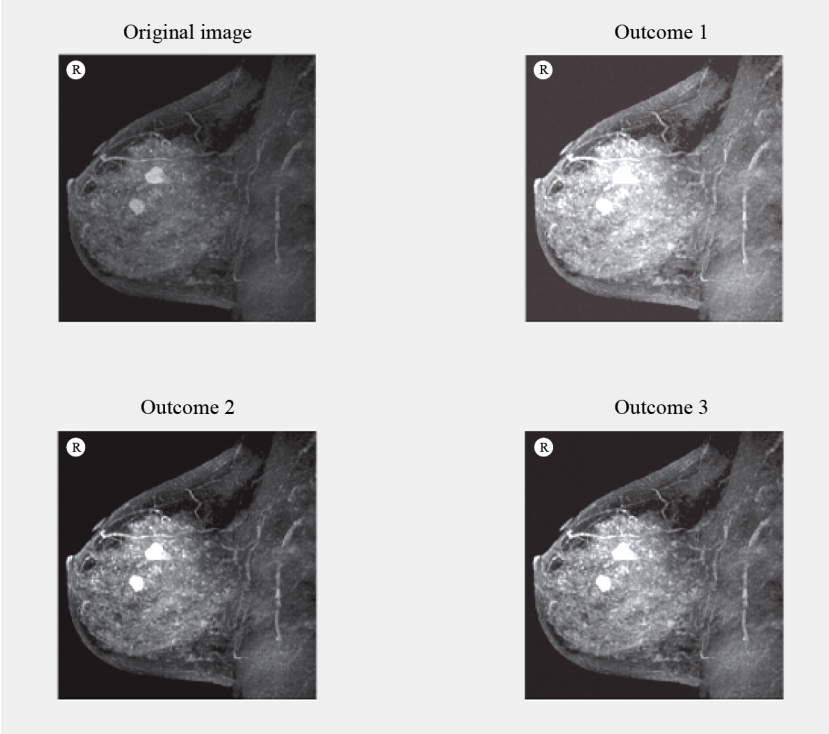

Figure 3. MRI of breast with malignant neoplasms image 3

Table 3. Values of the quality metrics obtained for different outcomes of image 3

Quality metrics	PSNR	SSIM	MSE	AMBE	Entropy
Power law transformation: Outcome 1	10.8697	0.0093	5.3224×10^3	65.0846	6.1080
Power law transformation: Outcome 2	10.8252	0.0032	5.3772×10^3	65.2859	6.1855
Power law transformation: Outcome 3	10.8375	0.0042	5.3620×10^3	65.2196	6.1723
Average	10.8441	0.0056	5.3538×10^3	65.1967	6.1553

4. Conclusion

The research's fundamental objective was to employ forefront medical imaging methods to improve our healthcare system's overall effectiveness and diagnostic potential. In particular, we investigated the effectiveness of power law transformation for gamma values larger than 1. We also presented a new technique for gamma value validation utilising the coefficients of the Sakaguchi type function in a domain with a Limacon shape. The choice of gamma values is supported by mathematics, as opposed to random assignment techniques. Our model's efficacy and distinctiveness are demonstrated by our comparative analysis with earlier research, which is referenced in references [11–16]. Our model had no known precedents. Our findings show that our method of image enhancement outperforms current methods in terms of quantitative performance indicators as well as visual quality with respect to [17–28]. Precise value analyses and improved graphics for each of the three test scenarios are used to display the results, which highlight the important function of power law transformation coefficients in DIP. This study opens the door to better diagnostic tools in medical imaging by shedding light on how these coefficients may significantly impact image quality. The works of [29–31] offers futuristic vision for further customising the current model.

5. Future scope

Adaptive coefficient selection: Based on the unique properties of the input image, future research can concentrate on creating adaptive algorithms that dynamically choose the best coefficients. This can improve the efficacy of image enhancement methods on a variety of medical image types, including X-rays, CT scans, and MRIs.

Machine learning integration: By automating the procedure and possibly enhancing accuracy and consistency, machine learning models can be trained to anticipate the best coefficients for power law transformation.

Acknowledgement

We would like to extend our heartfelt thanks to the anonymous reviewers for their thorough and constructive feedback, which significantly enhanced the quality of this manuscript.

Conflict of interest

The authors declare no competing financial interest.

References

[1] Ma WC, Minda D. A united treatment of some special classes of univalent functions. In *Proceedings of the Conference on Complex Analysis*. Tianjin; 1992. p.157-169.

[2] Raina RK, Sokół J. On coefficient estimates for a certain class of starlike functions, Hacet. *Journal of Mathematics and Statistics*. 2015; 44(6): 1427-1433.
[3] Murugusundaramoorthy G, Bulboacă T. Hankel determinants for new subclasses of analytic functions related to a shell shaped region. *Mathematics*. 2020; 8(6): 1041.
[4] Gandhi S. Radius estimates for three leaf function and convex combination of starlike functions. In *Mathematical Analysis I: Approximation Theory*. Singapore: Springer; 2020. p.173-184.
[5] Malik SN, Mahmood S, Raza M, Farman S, Zainab S. Coefficient inequalities of functions associated with petal type domains. *Mathematics*. 2018; 6(12): 298.
[6] Sharma K, Jain NK, Ravichandran V. Starlike functions associated with a cardioid. *Afrika Matematika*. 2016; 27: 923-939.
[7] Masih VS, Kanas S. Subclasses of starlike and convex functions associated with the Limaçon domain. *Symmetry*. 2020; 12(6): 942.
[8] Yuzaimi Y, Suzeini AH, Akbarally AB. Subclass of starlike functions associated with a limacon. *AIP Conference Proceedings*. 2018; 1974: 030023.
[9] Duren PL. *Univalent Functions*. New York: Springer; 1983.
[10] Grenander U, Szegö G. *Toeplitz Forms and Their Applications*. Berkeley: University of California Press; 1958.
[11] Senthilkumar B, Govindaswamy U. Breast cancer detection using combined curvelet based enhancement and a novel segmentation methods. *Biomedical papers of the Medical Faculty of the University Palacky, Olomouc, Czechoslovakia*. 2015; 159(1): 83-86.
[12] Gupta B, Mayank T. Minimum mean brightness error contrast enhancement of color images using adaptive gamma correction with color preserving framework. *Optik*. 2016; 127(4): 1671-1676.
[13] Sahoo S, Jagyanseni P, Mihir NM. Performance analysis of HE methods for low contrast images. *Procedia Computer Science*. 2016; 92: 72-77.
[14] Ali MH, Asaad FQ, Hamid AJ, Rabha WI. Breast cancer MRI classification based on fractional entropy image enhancement and deep feature extraction. *Baghdad Science Journal*. 2023; 20(1): 0221. Available from: https://doi.org/10.21123/bsj.2022.6782.
[15] Suradi SH, Kamarul AA. Digital mammograms with image enhancement techniques for breast cancer detection: a systematic review. *Current Medical Imaging*. 2021; 7(9): 1078-1084.
[16] Kurt B, Nabiyev VV, Turhan K. Comparison of enhancement methods for mammograms with performance measures. *Studies in Health Technology and Informatics*. 2014; 205: 486-490.
[17] Maitra IK, Nag S, Bandyopadhyay SK. Technique for preprocessing of digital mammogram. *Comput Methods Programs Biomed*. 2012; 107(2): 175-188.
[18] Hazarika M, Mahanta LB. A new breast border extraction and contrast enhancement technique with digital mammogram images for improved detection of breast cancer. *Asian Pacific Journal of Cancer Prevention*. 2018; 19(8): 2141-2148.
[19] Li JB, Wang YH, Tang LL. Mammogram-based discriminant fusion analysis for breast cancer diagnosis. *Clinical Imaging*. 2012; 36(6): 710-716.
[20] Oliver A, Freixenet J, Martí R, Zwiggelaar R. A comparison of breast tissue classification techniques. In *Medical Image Computing and Computer-Assisted Intervention-MICCAI 2006*. Berlin, Heidelberg: Springer; 2006. p.872-879.
[21] Singh S, Bovis K. An evaluation of contrast enhancement techniques for mammographic breast masses. *IEEE Transactions on Information Technology in Biomedicine*. 2005; 9(1): 109-119.
[22] Oliver A, Freixenet J, Martí J, Pérez E, Pont J, Denton ER, et al. A review of automatic mass detection and segmentation in mammographic images. *Medical Image Analysis*. 2010; 14(2): 87-110.
[23] Bellotti R, De Carlo F, Tangaro S, Gargano G, Maggipinto G, Castellano M, et al. A completely automated CAD system for mass detection in a large mammographic database. *Medical Physics*. 2006; 33(8): 3066-3075.
[24] Oliver A, Lladó X, Freixenet J, Martí R, Pérez E, Pont J, et al. Influence of using manual or automatic breast density information in a mass detection CAD system. *Academic Radiology*. 2010; 17(7): 877-883.
[25] Regentova E, Zhang L, Zheng J, Veni G. Detecting microcalcifications in digital mammograms using wavelet domain hidden Markov tree model. In *2006 International Conference of the IEEE Engineering in Medicine and Biology Society*. New York, NY, USA: IEEE; 2006. p.1972-1975.

[26] Mahdy AMS. Stability, existence, and uniqueness for solving fractional glioblastoma multiforme using a Caputo-Fabrizio derivative. *Mathematical Methods in the Applied Sciences*. 2023. Available from: https://doi.org/10.1002/mma.9038.

[27] Mahdy AMS. A numerical method for solving the nonlinear equations of Emden-Fowler models. *Journal of Ocean Engineering and Science*. 2022. Available from: https://doi.org/10.1016/j.joes.2022.04.019.

[28] Mahdy AMS, Lotfy K, El-Bary AA. Use of optimal control in studying the dynamical behaviors of fractional financial awareness models. *Soft Computing*. 2022; 26(7): 3401-3409.

[29] Mahdy AMS, Abdou MA, Mohamed DS. A computational technique for computing second-type mixed integral equations with singular kernels. *Journal of Mathematics and Computer Science*. 2024; 32: 137-151.

[30] Mahdy AMS, Nagdy AS, Hashem KM, Mohamed DS. A computational technique for solving Three-dimensional mixed volterra-fredholm integral equations. *Fractal and Fractional*. 2023; 7(2): 196.

[31] Al-Bugami AM, Abdou MA, Mahdy AMS. Sixth-kind chebyshev and bernoulli polynomial numerical methods for solving nonlinear mixed partial integrodifferential equations with continuous kernels. *Journal of Function Spaces*. 2023; 2023(1): 647649. Available from: https://doi.org/10.1155/2023/6647649.